

Zeitschrift: Helvetica Physica Acta

Band: 54 (1981)

Heft: 4

Artikel: Effect of the ponderomotive force in interaction of an amplitude modulated rf-field with a nonuniform plasma

Autor: Hoegger, B.A. / Schneider, H. / Vaucher, B.G.

DOI: <https://doi.org/10.5169/seals-115228>

Nutzungsbedingungen

Die ETH-Bibliothek ist die Anbieterin der digitalisierten Zeitschriften. Sie besitzt keine Urheberrechte an den Zeitschriften und ist nicht verantwortlich für deren Inhalte. Die Rechte liegen in der Regel bei den Herausgebern beziehungsweise den externen Rechteinhabern. [Siehe Rechtliche Hinweise.](#)

Conditions d'utilisation

L'ETH Library est le fournisseur des revues numérisées. Elle ne détient aucun droit d'auteur sur les revues et n'est pas responsable de leur contenu. En règle générale, les droits sont détenus par les éditeurs ou les détenteurs de droits externes. [Voir Informations légales.](#)

Terms of use

The ETH Library is the provider of the digitised journals. It does not own any copyrights to the journals and is not responsible for their content. The rights usually lie with the publishers or the external rights holders. [See Legal notice.](#)

Download PDF: 17.11.2024

ETH-Bibliothek Zürich, E-Periodica, <https://www.e-periodica.ch>

Effect of the ponderomotive force in interaction of an amplitude modulated *rf*-field with a nonuniform plasma*

B. A. Hoegger, H. Schneider and B. G. Vaucher, Department of Physics, University of Fribourg, CH-1700 Fribourg, Switzerland

(8. XII. 1981)

Abstract. Magnetoacoustic oscillations are excited in an inhomogeneous magnetized plasma cylinder by amplitude modulation of a high frequency field ($f_{rf} = 2.45$ GHz, $P_{rf} = 3$ kW PEP). The antenna is a long helical slow-wave structure. The axial field-oscillating with the modulation frequency ($f_{AM} = 2 \div 15$ MHz) – is monitored by means of electrostatically shielded magnetic probes. Resonance behaviour is observed around the eigenfrequency of the plasma cylinder. Power absorption is measured with diamagnetic loop technique. The plasma parameters are: Mean electron density $\bar{n}_e = 3 \cdot 10^{12}$ cm⁻³, electron temperature $T_e = 3.5$ eV, magnetic field $B_0 = 1.6$ kG, filling gas $p_0 = 7 \cdot 10^{-4}$ Torr argon.

I. Introduction

The interaction of intense radiation with a nonuniform plasma is at present a subject of general interest. The ponderomotive force is a well known effect in dielectrics [1] and similar formalism can be applied to a plasma. Bobin [2] recently reported on the ponderomotive pressure effects in laser driven high temperature plasma flows. When a high flux density of electromagnetic radiation impinges onto a plasma surface, energy and momentum can be transferred and nonlinear processes may take place. The nonlinear mechanisms in the coupling of strong em-waves are e.g. parametric decay, harmonic generation and ponderomotive force, usually obeying a power law.

By launching high power lower hybrid waves into a plasma with a phased waveguide array, Motley et al. [3] observed the generation of ponderomotive craters during the microwave irradiation. *RF*-pressure has been observed to modify the plasma density and surface. The ponderomotive force was introduced to the electron equation of motion by adding an *rf*-pressure term, depending on the amplitude of the external *rf*-electric field. In particular, when the wave impinges onto a linear density gradient with cutoff layer, a standing wave pattern is set up. Airy functions mathematically describe such structures [4].

A time dependent model, in which a linear density profile is modified by the ponderomotive force was investigated theoretically by several authors as e.g.

*) Supported by the Swiss National Science Foundation.

Morales and Lee [5], Washimi and Karpman [6], Sünder et al. [7] and Tskhakaya [8, 9]. Morales and Lee found in their analysis that at large pump strength, spatially localized electric fields appeared due to the self-generation of density cavities. With a simplified model they illustrated the basic effects caused by the modification of the density profile.

Recently, Wilson and Wong [10] presented an experimental study of the nonlinear coupling efficiency to lower hybrid waves from an external slow wave structure. Their results indicate that at high power the modification of the density profile near the antenna is due to the ponderomotive force, which can in fact drastically degrade the coupling between antenna and plasma.

The problem of coupling electromagnetic waves to a plasma is therefore of great interest since it offers the possibility of heating plasmas with readily available high-power gigahertz *rf*-sources.

In turn of the last years it has been paid much attention to the wave transmission by slow wave structures, see e.g. Bellan and Porkolab [11, 12] and Morales [13]. A comprehensive list of original literature can be found in a report of Musil et al. [14] on the retardation of electromagnetic waves by helices of large diameter.

In the present paper we wish to report on a new kind of experimental observation, in how the time dependent part of the ponderomotive force (see e.g. [8]) affects the nonlinear process in a magnetized plasma. We consider the interaction of an amplitude modulated *rf*-field, launched by a long helical slow-wave-structure. Hoegger et al. [15, 16] reported recently the first experimental evidence that magnetoacoustic waves can be excited by amplitude modulation of a high frequency em-wave ($\omega_{rf} \gg \omega_{AM}$). Resonance behaviour of the magnetoacoustic wave could be observed and will be described in more detail in this paper.

II. Experiment

Plasma production

The experimental arrangement is schematically shown in Fig. 1. A suitable microwave gun for preionization as described by Janzen et al. [17] and Musil et al. [18] is used. The plasma is generated by electron-cyclotron absorption (ECR) of the incident circular-polarized wave. The experimental device operates in the pulse regime ($\tau = 0.5 \div 1$ ms) with a repetition rate of 50 Hz. The preionization is carried out in a magnetic field B_1 , satisfying the ECR-condition for $f = 2.45$ GHz. In a subsequent *rf*-discharge in the homogeneous magnetic field region B_0 , the plasma is modified by two identical slow-wave structures to get steep radial gradients at the plasma boundary and a flat axial profile.

Absorption of the intense electromagnetic wave is monitored by measuring the reflected power of the wave. The mean electron density $\bar{n}_e = 3 \cdot 10^{12}$ cm⁻³ and the electron temperature $T_e = 3.5$ eV is measured using 8 mm MW-interferometer technique and Langmuir probes. The ion temperature is estimated by testwaves to be $T_i \approx 0.2$ eV. The density profile is measured in radial direction at different axial positions. The experiment described here is carried out in argon at a neutral gas pressure of $7 \cdot 10^{-4}$ Torr.

Figure 2 shows the radial electron density profile measured with Langmuir double probes in the midplane of the plasma column.

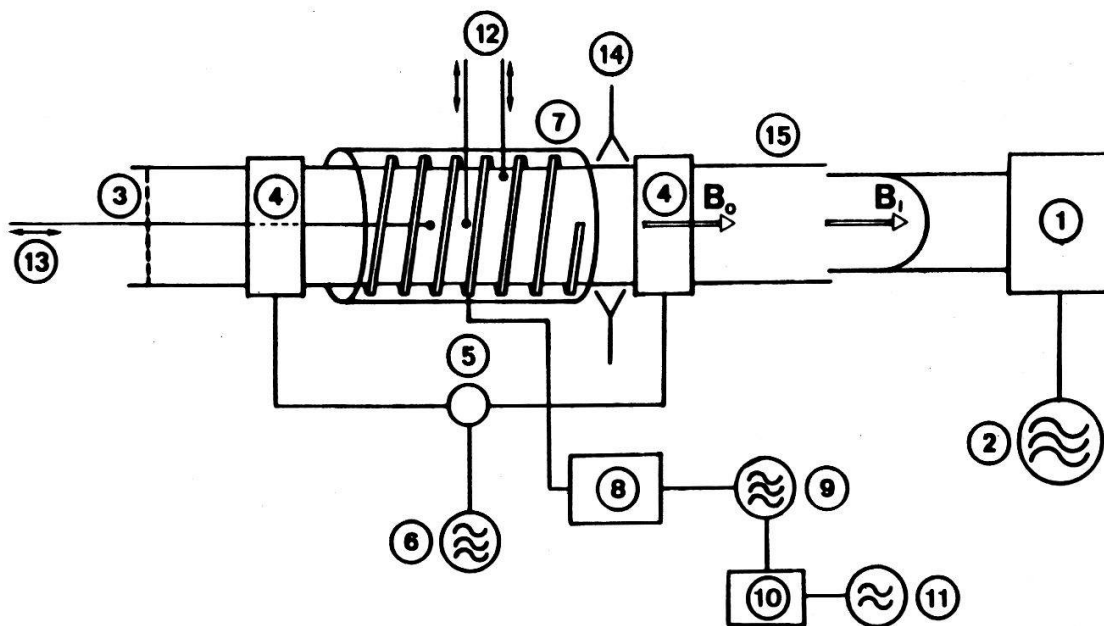


Figure 1
 Scheme of the experimental arrangement. 1. turnstile junction and coaxial waveguide antenna (TE_{11} -mode), 2. microwave generator, 3. grid, 4. slow wave structure for plasma production, 5. hybrid ring, 6. microwave generator, 7. antenna 8. impedance matching network, 9. magnetron, 10. amplitude modulation circuit, 11. rf -amplifier, 12. and 13. probes, 14. 8 mm MW-interferometer, 15. discharge tube (10 cm outer diameter, 100 cm length).

DENSITY PROFILE

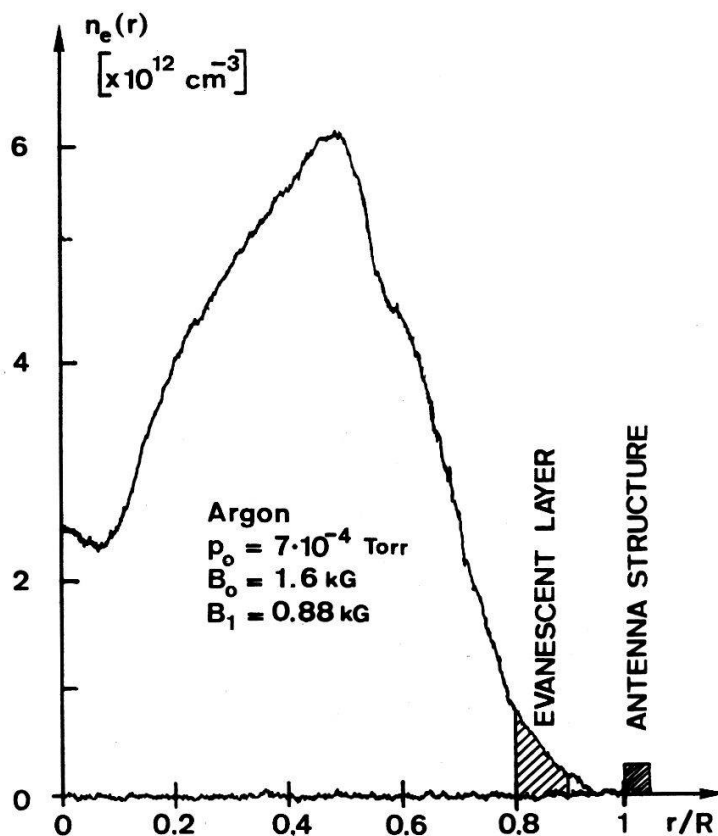


Figure 2
 Density profile $n_e(r)$: Plasma diameter $2R = 9.2 \text{ cm}$, Langmuir double probe: ion saturation current, $\bar{n}_e = 3 \cdot 10^{12} \text{ cm}^{-3}$ from 8 mm MW-interferometer.

Figure 3 shows typical experimental data for the time evolution of Langmuir-double-probe signals. Ion saturation current $I_{\text{isat}}(t)$, (top trace), radial probe position: $r/R = 0.5$; microwave interferometer signal $\bar{n}_e(t)$, (middle trace) and the timing of the amplitude modulated rf -wave burst, (bottom trace).

Antenna structure and RF-system:

A 50 cm long slow-wave structure in the central part of the homogeneous magnetic field is used as an antenna to couple the amplitude modulated microwave power to the plasma. A detailed schematic diagram of the electric circuit is shown in Fig. 4. The circuit consists mainly of an rf -amplifier ($P = 1$ kW, $f_{AM} = 2 \div 15$ MHz), the magnetron ($P = 2$ kW, $f_{rf} = 2.45$ GHz) and the timing circuit, for subsequent pulsing. Two magnetic field-probes, properly electrostatically shielded against direct pickup signals, are used for wave field measurements $\vec{B}_z(r, z)$.

III. The results of magnetoacoustic wave excitation

In excitation of electromagnetic waves with a slow wave structure, the most intense electric field is generated just inside the helical antenna. With an incident power $P_{RF} = 1 \div 3$ kW to the antenna, we estimate an electric field strength $E_{RF} \approx 150 \div 500$ V/cm between the antenna and the cutoff layer (see Fig. 2). This leads to a parameter $\langle E^2 \rangle / 8\pi nkT = 0.02 \div 0.4$ which is a measure of the RF to the plasma pressure.

In the cutoff layer the electron plasma frequency is: $f_{pe} = f_{RF} = 2.45 \cdot 10^9$ Hz, therefore the cutoff density is found to be $n_{ec} = 7.4 \cdot 10^{10} \text{ cm}^{-3}$. The temperatures are known to be: ($T_e \approx 20 T_i$); $T = T_e = 3.5$ eV.

With these edge plasma parameters, the ponderomotive force must be important and surface modification as manifested by steepening of the edge density gradient results.

If we modulate the amplitude of the applied microwave field in the magnetoacoustic range of frequencies, magnetoacoustic waves and resonances can be

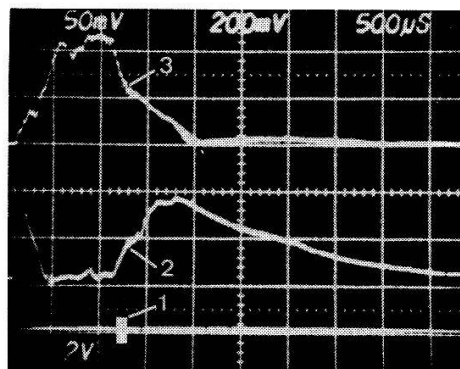


Figure 3

Plasma diagnostics and timing diagram. top trace: Langmuir double-probe, ion saturation current $I_{\text{ISAT}}(t)$; middle trace: 8 mm MW-interferometer; bottom trace: timing of the amplitude modulation burst in the afterglow of the plasma.

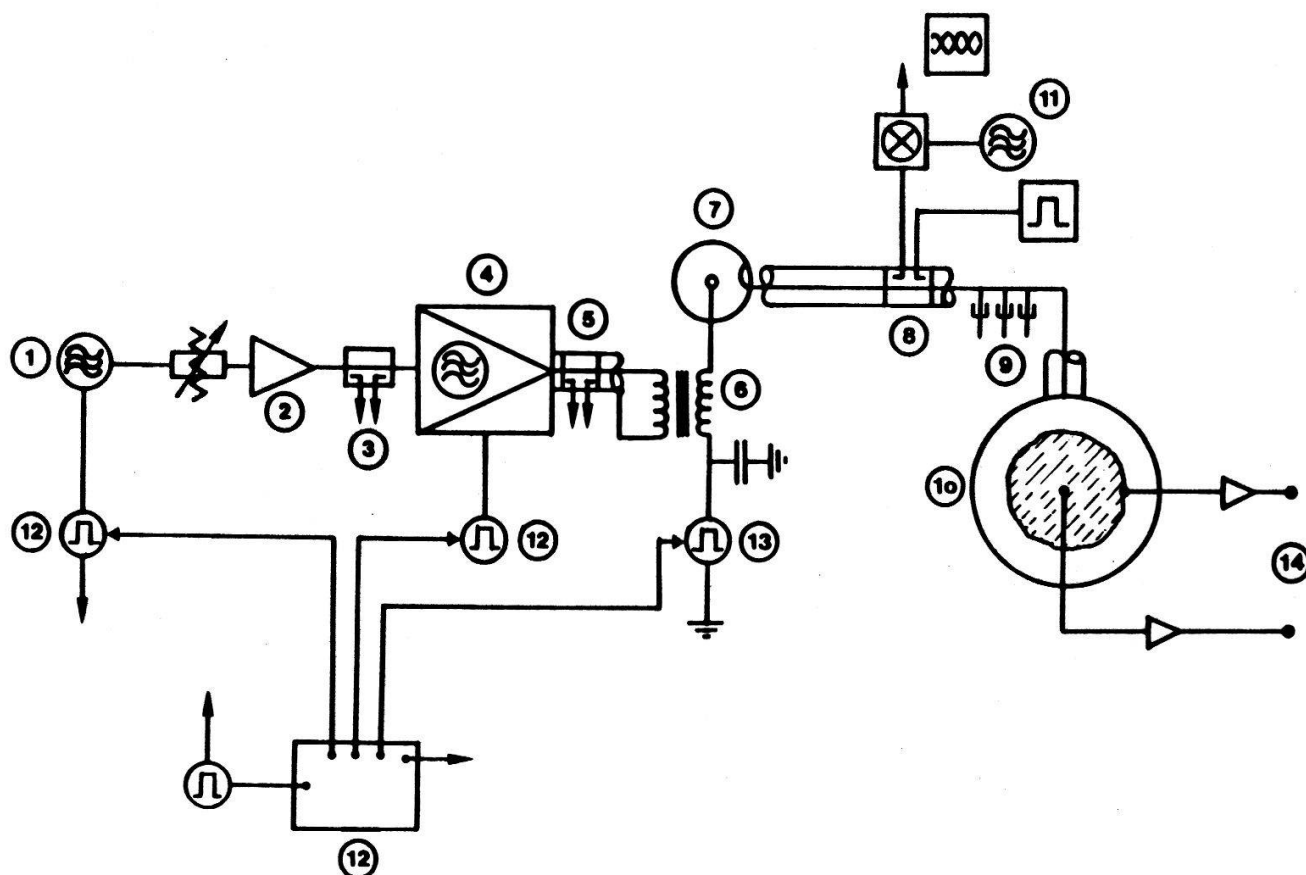
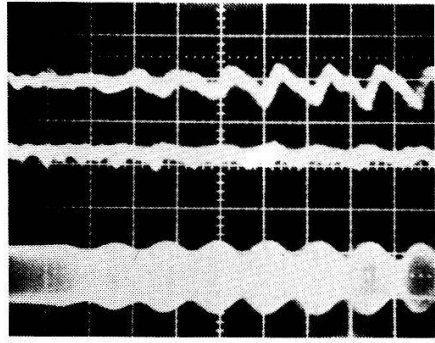


Figure 4

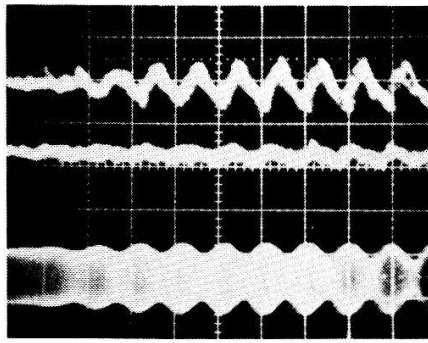
Circuit diagram of the amplitude modulated microwave generator and antenna system. 1. *rf*-sine wave generator, 2. broadband amplifier, 3. directional coupler, 4. *rf*-power amplifier, 5. directional coupler, 6. amplitude modulation transformer circuit, 7. magnetron, 8. directional coupler, 9. triple stub tuner, 10. slow wave antenna, 11. frequency downconversion circuit, 12. timing circuit, 13. *HV*-pulse circuit for magnetron, 14. *rf*-magnetic field probes.

expected. The eigenvalues – geometric resonances – in the nonuniform plasma cylinder are known from numerical calculations and previous experiments [19]. A computer code developed by R auchle [20] adapted to our problem was used.

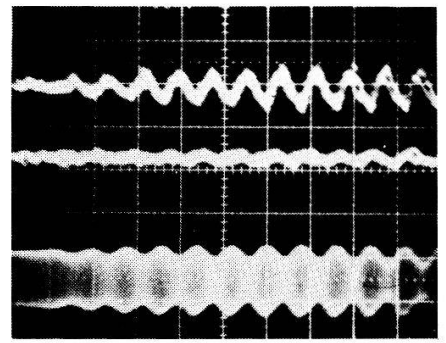
Figure 5 shows the amplitude modulated *rf*-field (bottom trace) applied to the plasma at different frequencies. The signal is monitored with a directional coupler for the incident power to the antenna and a frequency downconversion circuit, as shown in Fig. 4. The percentage of the amplitude modulation can be increased up to 80%. The magnetic field probe signals, which measure \tilde{B}_z ($r=0$) and \tilde{B}_z ($r=R$) are shown in the top and middle traces respectively. The oscillograms show a clear magnetic field oscillation \tilde{B}_z at exactly the respective modulation frequency, confirming the existence of magnetoacoustic waves. Measurements of the relative phase shift of the two signals, using Boxcar-technique (see e.g. Ref. [21]), for different modulation frequencies, approve the expected resonance behaviour. Looking at frequencies between $f_{AM} = 6$ to 10 MHz, a clear enhancement of the oscillating magnetic field in the center of the plasma is observed. This confirms the magnetoacoustic resonance behaviour predicted at these frequencies by numerical calculations, taking into account the strong inhomogeneity of the plasma cylinder. At higher modulation frequencies ($f_{AM} = 10 \div 15$ MHz), the signal behaviour is not yet well understood. Further investigation will decide whether the finite length of the plasma cylinder plays an



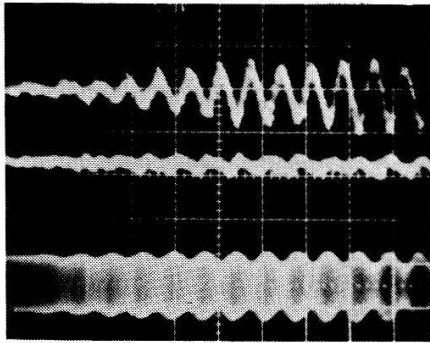
4 MHz



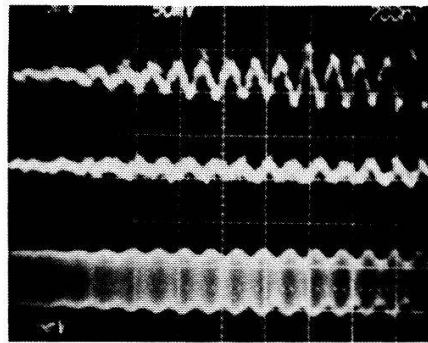
5 MHz



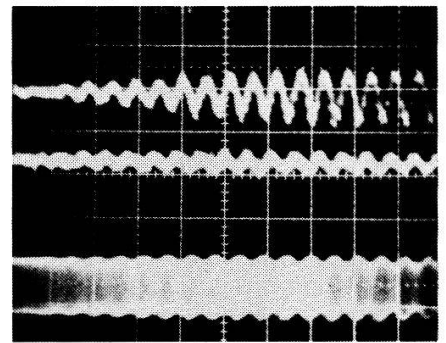
6 MHz



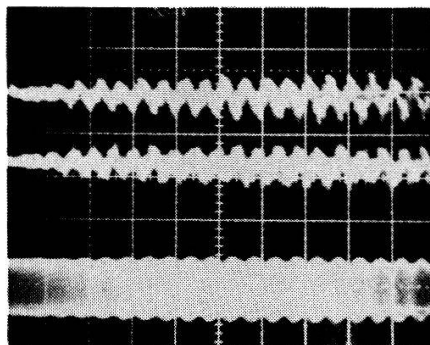
7 MHz



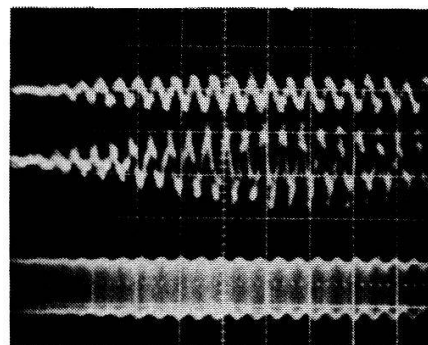
8 MHz



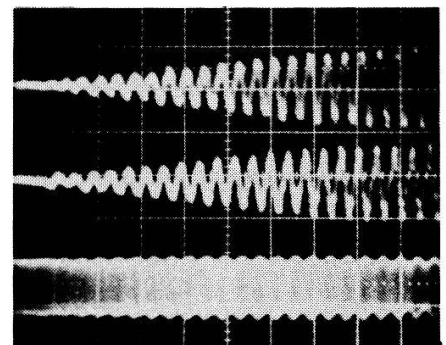
9 MHz



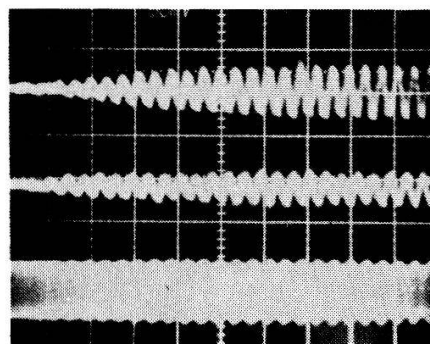
10 MHz



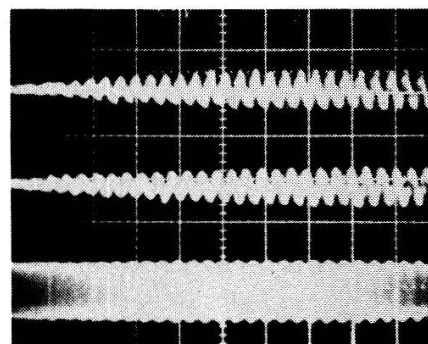
11 MHz



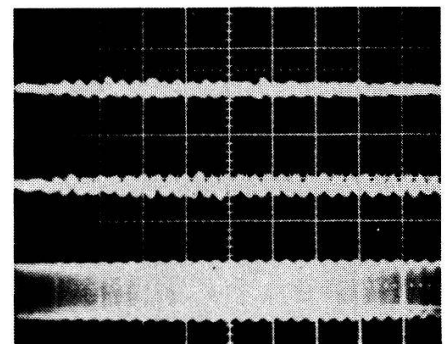
12 MHz



13 MHz



14 MHz



15 MHz

Figure 5

The results of magnetoacoustic wave excitation. bottom trace; amplitude modulated rf -field applied to the plasma at different frequencies. middle trace: wave field $\tilde{B}_z (r=0)$ and top trace: wave field $\tilde{B}_z (r=R)$.

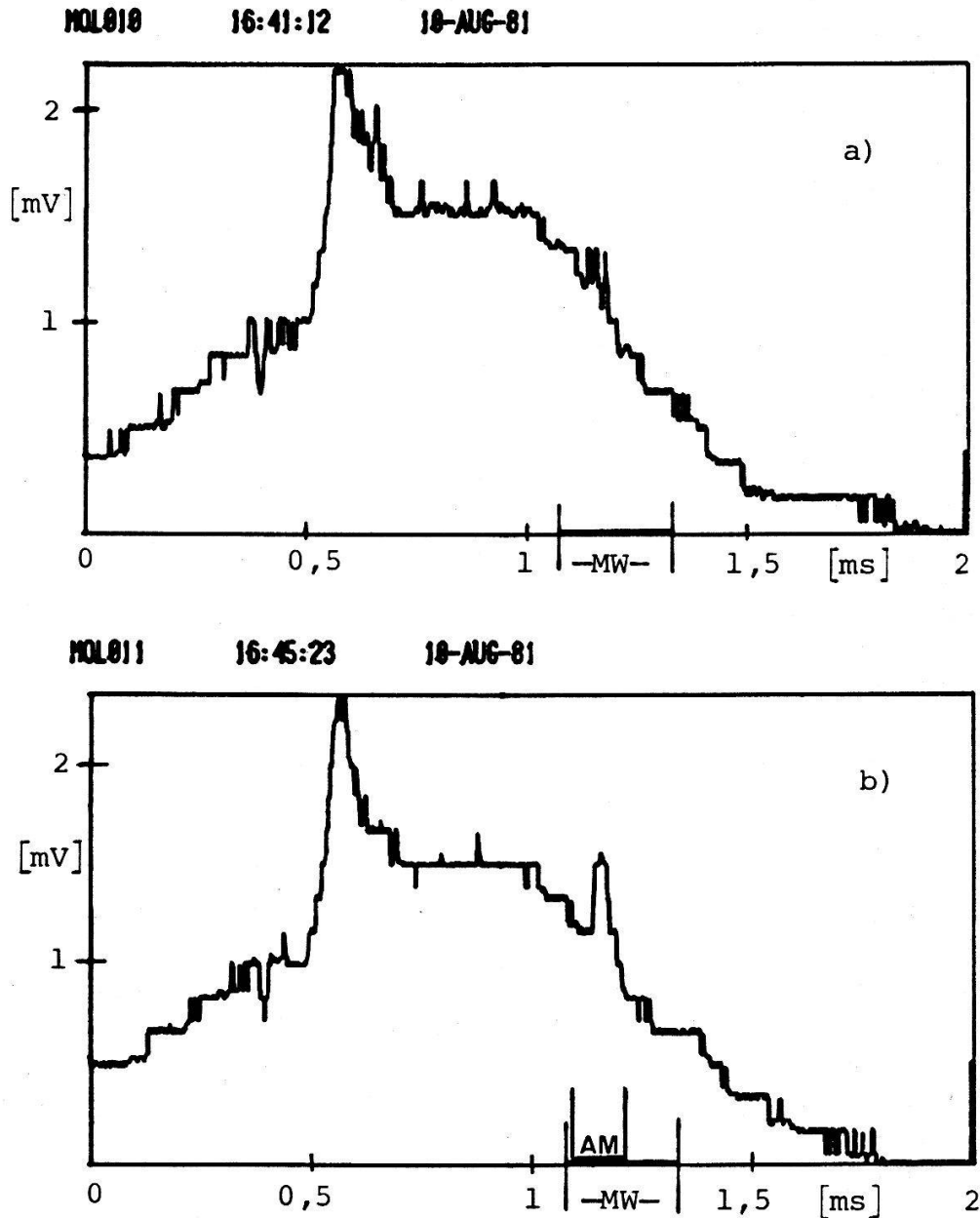


Figure 6

Wave absorption. Time response of the diamagnetic loop during the plasma production and magnetoacoustic wave excitation:

(a) without amplitude modulation of the microwave burst; MW-burst: $\Delta t_{MW} = 0.25$ ms

(b) with amplitude modulation ($f_{AM} = 8$ MHz) of the MW-burst, $\Delta t_{AM} = 0.15$ ms, percentage of modulation: 50%.

important role on the resonance behaviour, analogical to recent results of Grosse and Kraemer [22].

IV. Wave absorption measurements

Wave absorption or heating of the plasma is measured in the following way: A diamagnetic loop in its simplest form, consisting of $N = 2 \times 50$ turns of wire encircling the cylindrical plasma column, 10 cm apart from one end of the slow wave antenna measures the rate of change of magnetic flux within the plasma.

The balanced type loop is properly shielded against direct pickup signals and high common mode rejection is guaranteed by a fast differential operational amplifier (see Ref. [21]). Subsequently, the probe signal is integrated with an RC -circuit. The diamagnetic signal or transverse plasma pressure $p_{\perp} = nk(T_e + T_i)_{\perp}$ is given by the following expression:

$$p_{\perp}[\text{eV} \cdot \text{cm}^{-3}] = \bar{n}_e T_{e_{\perp}} = 5.0 \cdot 10^{18} \cdot \frac{\tau B_0}{N \cdot A} \cdot U_c \quad \text{for } T_e \gg T_i;$$

where \bar{n}_e is the mean electron density, $T_{e_{\perp}}$ is the transverse electron temperature, τ the integration constant $RC = 1.5 \cdot 10^{-3}$ [sec]. A is the plasma cross-section [cm^2], N the number of turns, B_0 [Gauss] the axial magnetic field and U_c the integrated diamagnetic signal [Volts]. Figure 6 shows two typical diamagnetic signals from the described loop circuit, recorded with a Biomation Type 8100 fast transient recorder, at a sampling rate of 1 MHz. The signal is subsequently processed with a PDP 11/34 mini computer system to subtract the background signal stemming from variations in the B_0 -field due to a ripple in the dc-current power supply. The signals are displayed by an XY-plotter. Trace (a) shows the diamagnetic signal of the target plasma with a subsequent microwave burst, $\Delta t = 0.25$ ms, in the afterglow of the target plasma. The signal shows only a very slight enhancement of the plasma diamagnetism, also the 8 mm MW-interferometer trace and the Langmuir double probe signal, monitored simultaneously, show no visible change.

As the microwave burst is amplitude modulated at frequencies in the range of magnetoacoustic resonance, the loop signal shows a clear enhancement of the plasma diamagnetism, confirming absorption of rf -energy. The peak shows the characteristic time delay resulting from finite transit time and a characteristic shape due to poor plasma confinement, inherent to linear plasma devices. The Langmuir double probe and MW-interferometer signal (arrow 3 and arrow 2 in Fig. 3) shows no increase of the electron density during the rf -burst. So the energy from the em-field to the plasma during the amplitude modulation (arrow 1 in Fig. 3) increases the plasma temperature.

V. Conclusion

We have observed experimentally for the first time that by amplitude modulation of a microwave field, launched by a helical slow wave antenna in the magnetoacoustic range of frequencies, magnetoacoustic waves and resonances can be excited.

We find an enhanced power absorption during the amplitude modulation phase of the microwave field, which seems to be considerable. Wave field distribution measurements, which shall elucidate the coupling mechanism will be the subject of further investigations.

REFERENCES

- [1] L. D. LANDAU and E. M. LIFSHITZ, *Electrodynamics of Continuous Media*, Pergamon (1960).
- [2] J. L. BOBIN, *J. Plasma Physics* 25, (1981), 193.
- [3] R. W. MOTLEY, W. M. HOOKE and C. R. GWINN, *Physics Letters* 77A, (1980) 451.

- [4] V. L. GINZBURG, *Propagation of Electromagnetic Waves in Plasma*, North Holland Publ. Comp. (1960), Amsterdam.
- [5] G. J. MORALES and Y. C. LEE, Report Dpt. of Phys. Univ. of California, Los Angeles, PPG-180, July 1974.
- [6] H. WASHIMI and V. I. KARPMAN, Soc. Phys. JETP 44, (1976), 528.
- [7] D. SÜNDER, V. S. PAVERMAN, N. L. TSINTSADZE and D. D. TSKHAKAYA, Soc. J. Plasma Physics 6, (1980), 90.
- [8] D. D. TSKHAKAYA, J. Plasma Physics 25, (1981), 233.
- [9] V. I. BEREZHIANI, V. S. PAVERMAN and D. D. TSKHAKAYA, Sov. J. Plasma Physics 6, (1980), 446.
- [10] J. R. WILSON and K. L. WONG, Princeton University Report, PPPL-1654, April 1980.
- [11] P. M. BELLAN and M. PORKOLAB, Phys. Fluids 17, (1974), 1592.
- [12] P. M. BELLAN and M. PORKOLAB, Phys. Rev. Lett. 34, (1975), 124.
- [13] G. J. MORALES, Phys. Fluids 20, (1977), 1164.
- [14] J. MUSIL, J. PREINHALTER and F. ZACEK, Report Institute of Plasma Physics, Czechoslovak Academy of Sciences, Prague, CSSR.
- [15] B. A. HOEGGER, H. SCHNEIDER, B. G. VAUCHER and G. KÜHNE, Physics Letters 86A, (1981), 149.
- [16] B. A. HOEGGER, H. SCHNEIDER, B. G. VAUCHER and G. KÜHNE, Bull. Am. Phys. Soc. 26, (1981), 888.
- [17] G. JANZEN and E. RÄUCHLE, Physics Letters 83A, (1981), 15.
- [18] J. MUSIL and F. ZACEK, Czech. J. Phys. B20, (1970), 337.
- [19] B. A. HOEGGER, Ch. RITZ, H. SCHNEIDER and B. G. VAUCHER, Physics Letters 76A, (1980), 393.
- [20] E. RÄUCHLE, University of Stuttgart, Report IPF-72-8.
- [21] H. SCHNEIDER, B. A. HOEGGER, Ch. RITZ, B. G. VAUCHER and T. M. TRAN, Helvetica Physics Acta 53, (1980), 40.
- [22] K. GROSSE and M. KRÄMER, Physics Letters 86A, (1981), 152.